Photographic studies of laser-induced bubble formation in absorbing liquids and on submerged targets: implications for drug delivery with microsecond laser pulses

HanQun Shangguan, MEMBER SPIE
Oregon Medical Laser Center
9205 S.W. Barnes Road
Portland, Oregon 97225
E-mail: hanquan@ee.pdx.edu

Lee W. Casperson*
University of Rochester
The Institute of Optics and The Rochester Theory Center for Optical Science and Engineering
Rochester, New York 14627

Dennis L. Paisley, MEMBER SPIE
Los Alamos National Laboratory
MS P952 Group DX-1
P.O. Box 1663
Los Alamos, New Mexico 87545

Scott A. Prahl
Oregon Medical Laser Center
9205 S.W. Barnes Road
Portland, Oregon 97225
and
Oregon Health Sciences University
Portland, Oregon 97201

Abstract. Pulsed laser ablation of blood clots in a fluid-filled blood vessel is accompanied by an explosive evaporation process. The resulting vapor bubble rapidly expands and collapses to disrupt the thrombus (blood clot). The hydrodynamic pressures following the bubble expansion and collapse can also be used as a driving force to deliver clot-dissolving agents into thrombus for enhancement of laser thrombolysis. Thus, the laser-induced bubble formation plays an important role in the thrombus removal process. We investigate the effects of boundary configurations and materials on bubble formation with time-resolved flash photography and high-speed photography. Potential applications in drug delivery using microsecond laser pulses are also discussed. [S0091-3286(98)00108-1]

Subject terms: laser-induced cavitation bubble; localized drug delivery; high-speed photography; hydrodynamic pressure.

Paper HSP-01 received Jan. 6, 1998; accepted for publication Mar. 15, 1998.

1 Introduction

Interest in cavitation bubbles in liquids initially arose from their destructive action on ship propellers and in hydraulic machinery. Cavitation erosion is attributed to the action of acoustic transients emitted during bubble collapse and to the impingement of the high-speed liquid jet that develops when a bubble collapses in the vicinity of a solid boundary.[1] It was shown soon after the invention of the laser that cavitation can also occur in a liquid when irradiated with pulsed laser light.[2] This form of cavitation is called optical cavitation.

Laser-induced cavitation bubbles have been used in ophthalmology, urology, and cardiology. For example, laser pulses produce a plasma with subsequent bubble formation for ocular surgery by photodisruption.[3] Laser lithotripsy fragments kidney stones through cavitation erosion.[4] Laser pulses have been used to remove thrombus in obstructed arteries.[5] In a previous study, we demonstrated that the laser-induced hydrodynamic pressures arising from cavitation bubble expansion and collapse could also drive drug into the thrombus.[6] This technique is termed photomechanical drug delivery.[7] It has been found that the cavitation bubble formation is the governing mechanism for this technique.

A cavitation bubble can be generated at a fiber tip or on an ablation target, depending on where the laser energy is absorbed. The cavitation bubble is formed at the fiber tip when a laser pulse is delivered into an absorbing liquid (e.g., blood). The bubble can also be formed on a submerged target (e.g., blood clot) if a fluid-core catheter is used to wash away ambient blood, and, for example, a 480 or 577 nm laser pulse can be absorbed by the blood clot.[8,9]

Although several studies have focused on the laser-induced cavitation bubble dynamics,[10–12] little work has been done on the dynamic behavior of laser-induced cavitation bubbles formed in absorbing liquids with different physical properties or on ablation targets with different mechanical strengths with the pulsed dye laser. The aims of this study are

1. to study the boundary effects of the fiber and container on the bubble formation to simulate the effect of clinically relevant boundary conditions (vessel walls and laser catheter) on cavitation bubble formation
2. to investigate the material effects on the bubble for-

*Permanent address: Portland State University, Department of Electrical Engineering, P.O. Box 751, Portland, Oregon 97207-0751.

mation; specifically, how the different liquids surrounding a fiber tip or on a target surface affect the bubble formation and also how mechanical strength of thrombus affects the bubble dynamics.

2 Materials and Methods

2.1 *Sample Preparations*

2.1.1 *Absorbing liquids*

Two liquids (water and mineral oil from Paddock Lab) were used in this study. Dyes (Direct Red 81 from Sigma and D&C Red no. 17 from Warner-Jenkinson) were added to water and oil, respectively, to achieve the desired absorption. Both of these dyes were photostable and had a peak absorption around 504 nm. The absorption coefficients of the solutions had a nearly linear relationship with the concentration of dye in the solutions: 0.0837 g of Direct Red 81 in 30 mL water gave an absorption coefficient of 300 cm^{-1}, while 0.0367 g of D&C Red no. 17 was added into 30 ml oil to obtain the same absorption. Direct Red 81 dye was easily dissolved in water after stirring several minutes at room temperature ($\sim$25°C). Heating was needed to make the oil solutions. The dye-oil mixture was heated to 100°C with stirring until the appearance became uniform, and it was then cooled down to room temperature before the experiments.

2.1.2 *Absorbing soft targets*

Thrombus was simulated using 3.5 to 5% gelatin (60 to 300 bloom, Sigma Chemicals). The percentage was determined by the weight ratio of gelatin to water. The bloom number is the standard method for indicating the toughness of gelatins and is a measure of surface tension. Higher bloom numbers indicate stronger gelatins. No attempt was made to correlate the bloom number with the strength of any specific clots in this study, although the range studied was similar to that of typical clot toughness. The gelatin-water mixture was heated to 60°C with stirring until it became clear. Liquid gelatin samples were poured into 1-cm cuvettes and molded to form 2 to 3 cm-thick thrombus models with flat surfaces. Dye solution (0.07 g of Blue 15 from Sigma in 40 mL water) was placed on the gelatin surface for 5 min and a blue layer ($\sim$300 μm thick with an $\sim$100 cm^{-1} absorption coefficient at 577 nm) was formed. This blue layer enabled the boundaries of the cavitation bubble to be seen, even when they otherwise would have been hidden by a light absorbing gelatin substrate. At 504 nm, 300 cm^{-1} gelatin samples were made by adding 0.3 g of Direct Red 81 from Sigma in 100 mL of liquid gelatin (3.5% 175 bloom).

2.2 *Laser Irradiation*

Laser irradiation at 504 or 577 nm was provided by flashlamp-excited dye lasers (Palomar Medical Technologies). The pulse duration was $\sim$1.3 μs (full width at half maximum). The laser pulses were delivered into absorbing liquids or through clear liquids onto thrombus phantoms via a fused-silica fiber with 300 or 1000 μm diameter. The energy per pulse was measured with a joulemeter (Molectron). Pulse-to-pulse energy variation was less than 5%.

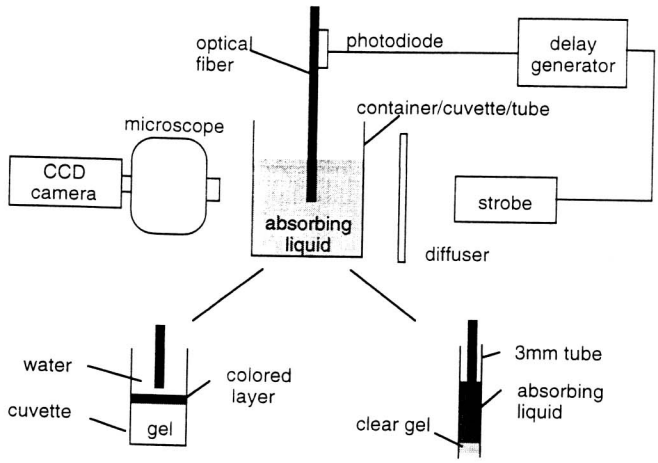

Fig. 1 Schematic of experimental setup for flash photography.

2.3 *Photographic Systems*

Two photographic systems were used to visualize the bubble formation. A time-resolved flash photographic setup provided a series of single stroboscopic pictures, while a high-speed framing camera captured 12 images for a single event. The bubble sizes were measured directly from the images by using the optical fiber in each image as a scale factor. The images were analyzed using NIH Image or IP Lab software.

2.3.1 *Flash photography*

The microsecond time-resolved flash photography setup is shown in Fig. 1. The processes taking place at the fiber end or on the gelatin surface were photographed using a triggerable CCD camera (CV-251, Protec). A stereomicroscope (SZ60, Olympus) was used for magnification. Each picture was a single event and was repeated three times for each parameter set. The bubble size was reproducible to 5% before the bubble collapse. The appearance of the cavitation bubbles varied widely after the bubble collapse. A strobe (MVS–2601, EG&G) with a 5 μs pulse duration (full width at half maximum) was used for illumination. The delay times were controlled by a digital delay generator (DG535, Stanford Research Systems). The generator was triggered by the laser pulse by using a photodiode (UDT Instruments) that was attached to the laser delivery fiber, and flash photographs were taken at variable delay times of 5 to 500 μs after the laser pulse. A laser filter was positioned in front of the microscope to avoid blinding the CCD camera.

2.3.2 *High-speed shadowgraph*

Figure 2 shows a schematic of the high-speed photographic system. A cw argon ion laser at 514 nm was used for illumination. The argon beam was expanded to 10 mm diameter using a 3× beam-expanding telescope for illuminating the sample area. A shadowgraph of the sample surface and optical fiber was imaged on the input of an electronic framing camera (FS501, Ultranac). By properly timing the pulsed-dye laser and argon ion laser with the triggering of the electronic framing camera, multiple exposures of the interaction of the laser pulse with the thrombus could be

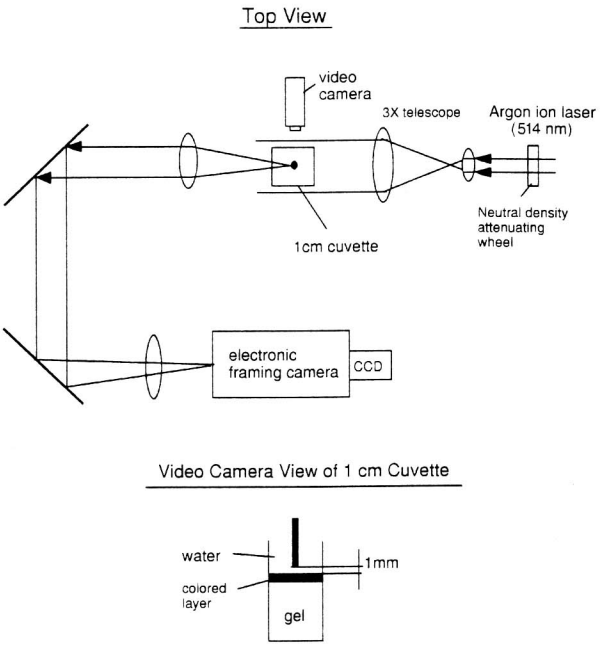

Fig. 2 Schematic of high-speed shadowgraph system.

realized. The ablation process could be examined from as early as several hundred nanoseconds to several hundred microseconds after the laser pulse. The electronic framing camera captured 12 pictures with an adjustable interframe time. The photographs were taken with 1 μs exposure time and 25 μs interframe time. The 12 frames were captured on a 1152 × 770 pixel CCD chip with the image read directly into a PC for data analysis. The illumination light was adjusted using a neutral density wheel (50G00AV.2, Newport).

2.4 *Experiments*

2.4.1 *Boundary effect*

It has been shown that similar maximum cavitation bubble sizes can be produced by different sets of laser parameters.[6] For example, a cavitation bubble 3.2 mm in diameter can be produced in unbounded colored oil (300 cm^{-1}) by a 300 μm fiber at 33 mJ, by a 600 μm fiber at 50 mJ, or by a 1000 μm fiber at 100 mJ, with an error estimate of less than 5%. It is unclear, however, whether the bubble generated by a smaller fiber can produce the same hydrodynamic pressure as that created by a larger fiber with higher energy when the bubble diameters are similar. Thus, an experiment was performed in a silicone tube (3 mm inner diameter and a wall thickness of 0.4 mm) as a blood vessel model using energies that could create bubbles of the same width for a 300 μm fiber and a 1000 μm fiber. The mechanical properties of the silicone tube differed from those of human arteries; the Young's modulus of the silicone tube was 8 N/mm^2, whereas it is 2 to 5 N/mm^2 for human vessels.[13] The effects of boundaries were also investigated by comparing the bubble dimensions generated in absorbing liquids with different boundary conditions (i.e., a 52 × 52 × 50 mm bottle and 3-mm silicone tube).

Table 1 Variation in maximum bubble size when formed in 300-cm^{-1} liquids or under clear liquids on 300-cm^{-1} gelatin.

Liquid	Density (mg/mm^3)	Viscosity (cP)	Bubble Width: In Liquid (mm)	Bubble Width: On Gelatin (mm)
Water	0.992	0.653	3.9	5.5±0.2
Mineral oil	0.86	29.67	2.2	5.4±0.2
Contrast medium	1.411	13.34	—	5.2±0.3

Note that the bubbles formed in liquids were confined by a 3-mm tube, and consequently are smaller than bubbles formed in 1-cm cuvettes because of the presence of tube boundaries. The errors are the standard deviation of three measurements.

2.4.2 *Material effect*

Three experiments were performed to investigate the effects of materials:

1. Does the viscosity and density of absorbing liquids affect the size of bubbles formed in the liquids?
2. What are the differences when the bubble forms on a soft target immersed in the liquids?
3. Does the mechanical strength of the ablation targets affect the bubble dynamics?

In the first experiment, single pulses of 100 mJ were delivered into an oil solution or water solution through a 1000 μm fiber. The absorption coefficient for both solutions was 300 cm^{-1}. The solutions filled a 3 mm-diameter silicone tube and the fiber was centered inside the tube. The laser emitted light with a wavelength of 504 nm.

In the second experiment, two sets of experiments were performed. The first set used single pulses of 50 mJ delivered onto 100 cm^{-1} gelatin through clear water or clear oil via a 300 μm fiber placed 1 mm above the gelatin surface. The bubble formation was visualized using flash photography and high-speed shadowgraphy. The laser emitted 577 nm light. The second set used 100 mJ laser pulses to irradiate the gelatin sample (300 cm^{-1}) through clear water, clear mineral oil (USP, Paddock Lab), and clear contrast medium (MD-76, Mallinckrod Medical, Inc.) using a 1000 μm fiber that was 1 mm away from the gelatin surface. The bubble width was measured 300 μs after the laser pulse with flash photography. The laser operated at 504 nm. The density and viscosity for water, mineral oil, and contrast medium are summarized in Table 1.

The third experiment visualized the bubble formation on 100 cm^{-1} gelatin with different mechanical strengths. Single pulses of 50 mJ were delivered via a 300 μm fiber onto a gelatin sample (100 cm^{-1}) with varied hardness (3.5% 60 bloom and 5% 300 bloom) under water. The fiber tip was 1 mm above the gelatin surface and centered inside the 1 cm cuvette. The laser operated at 577 nm.

3 Results

3.1 *Boundary Effect*

Figures 3 and 4 show the bubble evolution in a 300 cm^{-1} oil solution confined in a 3 mm silicone tube. The bubbles

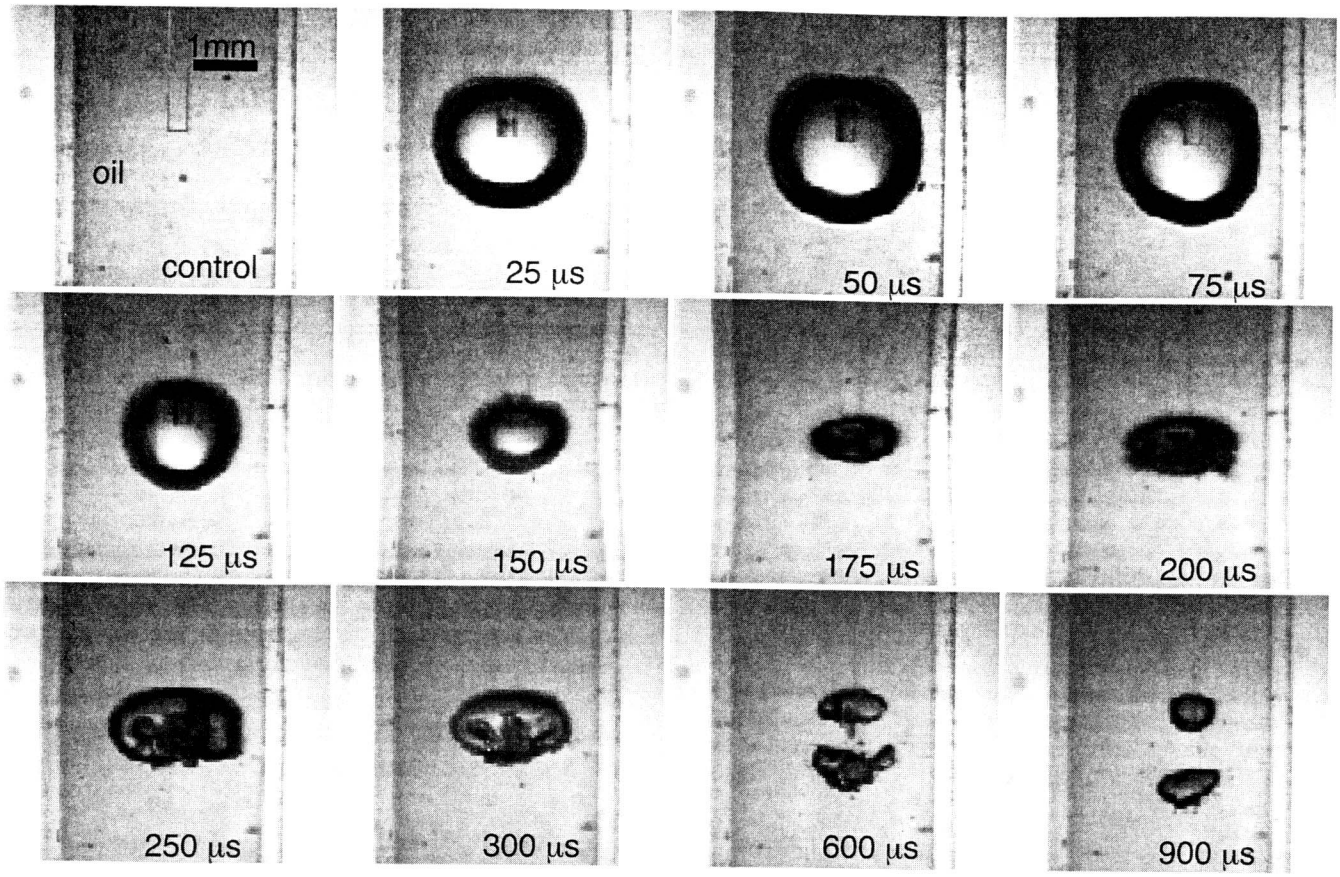

Fig. 3 Side view of bubble formation in a 300-cm^{-1} oil solution confined in a 3-mm silicone tube. Single pulse of 33 mJ was delivered via a 300-μm fiber.

were created by delivering single pulses of 33 mJ via a 300 μm fiber (Fig. 3) or 100 mJ via a 1000 μm fiber (Fig. 4), respectively. There were no differences in the maximal tube wall diameter due to the bubble expansion and minimal diameter caused by the collapse between the two cases. In both cases, the bubble reached its maximum size 50 μs after the laser pulse and dilated the tube wall by 10%. The subsequent bubble collapse caused a 4% invagination of the tube wall. Figure 5 shows the bubble expansion and collapse in an unbounded 300 cm^{-1} water solution (top panel) and in the silicone tube (bottom panel). The bright spot in the second frame (top panel) was the flash of light from the strobe. The maximal dilation of 29% was at 60 μs and the tube diameter was reduced by 16% at 900 μs due to the collapse.

3.2 *Material Effect*

The cavitation bubble dimensions were significantly different when the bubbles were formed in the 300 cm^{-1} oil solution (Fig. 4) compared with those formed in the 300 cm^{-1} water solution (Fig. 5). The maximum bubble width formed in the water solution was larger than that formed in the oil solution by a factor of 1.8 (i.e., 3.9 mm in water and 2.2 mm in oil) using the same laser energy (in this case, 100 mJ) and resulted in significant differences in the dilation and invagination of the tube wall.

Figure 6 shows the bubble width generated on the absorbing gelatin surface under clear water and oil. There were no significant differences in bubble sizes formed on the gelatin under water or oil. The bubble heights did not differ significantly from the widths. The bubble in water grew faster initially ($\sim$25 μs), while at 50 μs they had the same size. Flash photographs revealed that the bubble dimensions formed under water, oil, and contrast medium were quite similar to each other. The measurements are summarized in Table 1. We observed that a stream of color was released from the absorbing gelatin surface when the contrast medium interacted with the gelatin samples. This was not observed for water or oil.

Figures 7 and 8 show in side view the behavior of a bubble generated on an absorbing gel surface with different mechanical strengths using the flash photography setup. Two series of high-speed shadowgraphs are shown in Figs. 9 and 10. In the case of soft 3.5% 60 bloom gelatin, the bubble shape was spherical during expansion and contraction. The bubble reached its maximal dimension about 100 μs after the laser pulse, and then started to contract slowly (Fig. 7). The collapse occurred about 300 μs after the laser pulse. The bubble shape became elliptical between 150 and 200 μs after the laser pulse when the harder 3.5% 300 bloom gelatin was used (Fig. 8). The first collapse was observed at about 250 μs and then slightly rebounded. The second collapse occurred between 400 and 450 μs. The gelatin was ejected from the surface afterward. Similar bubble behavior was observed from the high-speed shadowgraphs. The bubble widths measured from Figs. 9 and

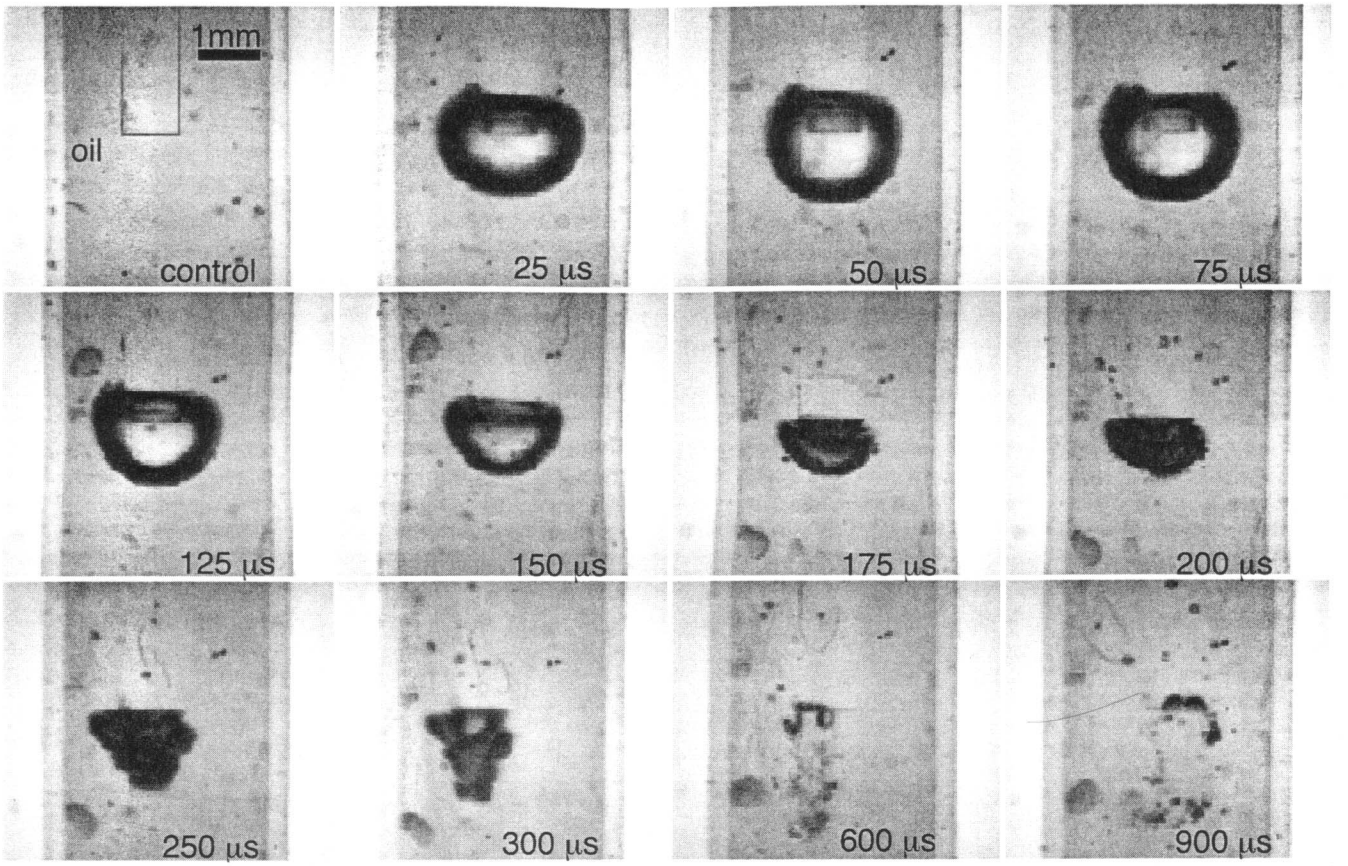

Fig. 4 Side view of bubble formation in a 300-cm^{-1} oil solution confined in a 3-mm silicone tube. Single pulse of 100 mJ was delivered via a 1000-μm fiber.

10 are plotted as a function of delay time in Fig. 11. These shadowgraphs confirmed that the series of isolated stroboscopic pictures could be used to characterize the bubble formation even though the process may vary from shot to shot and from sample to sample.

4 Discussion

We investigated the effects of boundary and materials on the bubble formation, which are of potential clinical interest, for photomechanical drug delivery in particular. To simulate the effect of clinically relevant boundary conditions (e.g., vessel walls and laser catheters) on the bubble formation, the absorbing liquids were confined in a 3 mm silicone tube as a vessel model and the laser light was delivered through optical fibers with different diameters. The use of liquids with different physical properties or gelatin samples with different mechanical strengths provided a simple way to elucidate how the materials affect the dynamic behavior of the bubbles in absorbing liquids and on soft targets, as may occur in the process of photomechanical drug delivery or laser thrombolysis *in vivo*. Two photographic techniques, time-resolved flash photography and high-speed shadowgraphy, were used to visualize the bubble formation. The bubble dimensions measured with both techniques were quite similar to each other, although the flash photographic setup provided a series of single stroboscopic pictures, while the high-speed framing camera captured 12 images for a single event. The differences were within 5%.

This study showed that bubbles of the same size could be created using different fibers with different energies. These equal sized bubbles had the same mechanical effects on dilation and invagination of a 3 mm silicone tube wall. This finding suggests that photomechanical drug delivery can be achieved by use of smaller fiber with lower energy. The results of the present study also demonstrated that the bubble formation was affected by the surrounding space. The bubbles formed in the semi-infinite medium, i.e., in a $52 \times 52 \times 50$ mm bottle, were larger than those formed in a 3 mm tube (Fig. 5). About 34% of the bubble energy was dissipated in the dilation of the tube wall. This estimation was made using Rayleigh's bubble formula[3,4,14]: $E_{\text{bubble}} = 4/3\pi R_{\text{max}}^3 \Delta p$, where E_{bubble} is the energy of the bubble and Δp is the difference between inner and outer pressure, by assuming $\Delta p = 1000$ kPa (the hydrostatic pressure) in both the plastic bottle and tube.

Photomechanical drug delivery uses the hydrodynamic pressure following the laser-induced bubble expansion and collapse to deliver the drug into the thrombus during the laser thrombolysis procedure. The bubble is formed on the thrombus covered with clear fluids (e.g., saline and contrast). One concern is whether the density and viscosity affect the bubble dynamics. This study demonstrated that

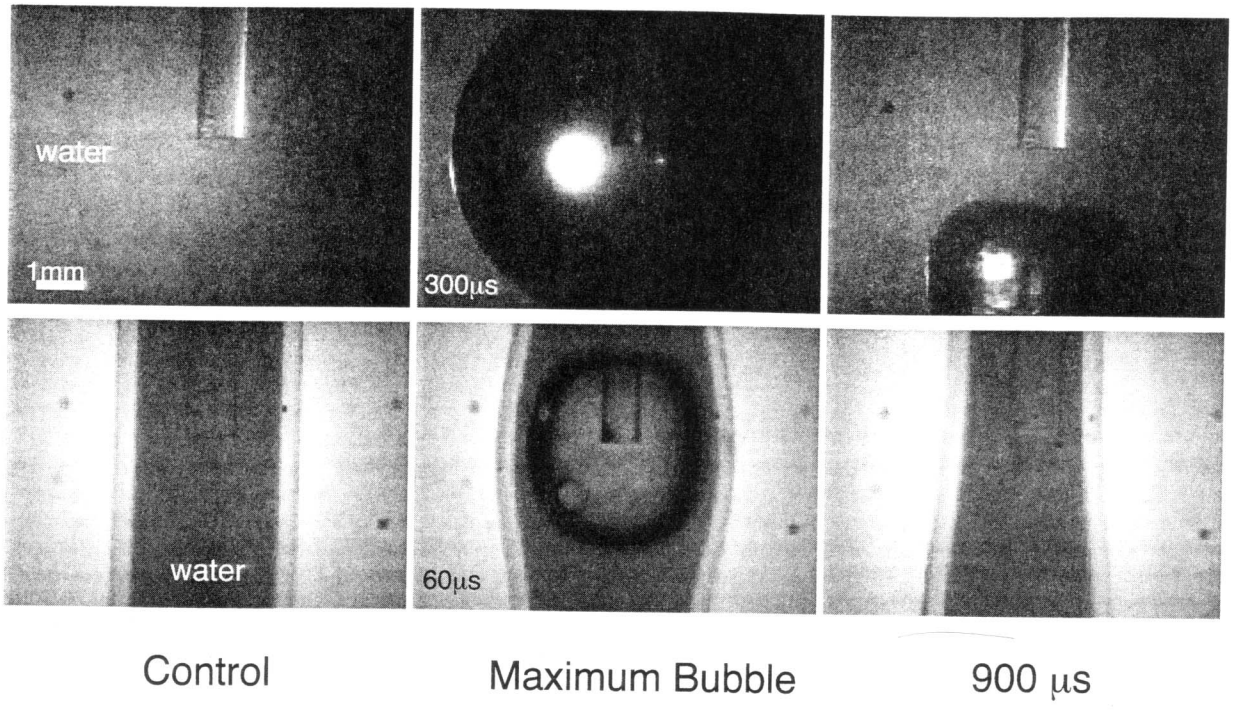

Fig. 5 Side view of bubble formation in a semi-infinite space (top panel) and in a 3-mm tube (bottom panel). Single pulses of 100 mJ were delivered into a 300-cm^{-1} water solution via a 1000-μm fiber. The maximal bubble diameter and dilation of the tube wall were observed at 300 and 60 μs, respectively, after the laser pulse. The invagination of the tube was 84% of the initial value about 900 μs after the laser pulse.

the effects of density and viscosity of the liquids above the target on the bubble formation are negligible when the bubble is formed on an ablation target (Fig. 6 and Table 1), but the bubble dynamics strongly depended on the physical properties of the absorbing liquid when the bubble is formed in an absorbing liquid (Figs. 4 and 5). These findings suggest that the properties of the liquids dominate the bubble formation as the laser energy is absorbed by the absorbing liquids, while the bubble formation is governed by the properties of the targets if the laser energy is absorbed by the target. In brief, the dynamics of bubble formation depends on where the bubble is formed. Moreover, photomechanical drug delivery may be achieved by using any drugs that are suitable for dissolving the thrombus during laser thrombolysis regardless of the density and viscosity of the drug.

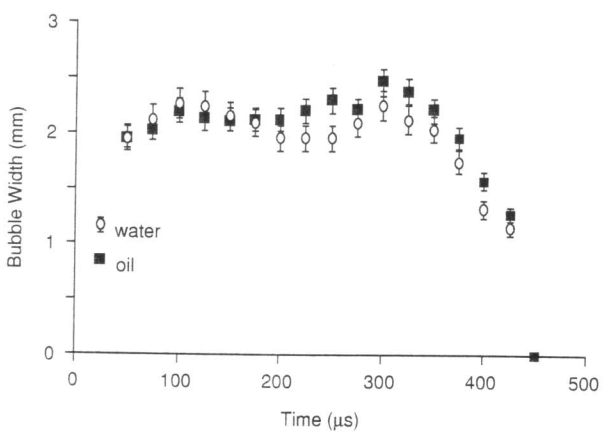

Fig. 6 Measured bubble diameter as function of time. Single pulses of 50 mJ were delivered onto the absorbing gelatin surface (100 cm^{-1}) through clear water and oil via a 300-μm fiber. The fiber tip was 1 mm above the gelatin surface. Error bars represent the standard deviation of three measurements.

The flash photographs revealed that larger bubbles formed in water could cause greater dilation of the tube wall (Figs. 4 and 5). A study by de la Torre and Gregory suggested that laser-induced cavitation bubbles could cause dissections in vascular tissue during pulsed-dye laser angioplasty.[15] Reducing bubble dimensions has been proposed to minimize the dissections.[11,12,16] This study suggests that the bubble size may be reduced by using a liquid such as oil in which small bubbles are formed rather than water.

Previous studies have demonstrated that the mechanical properties of tissue significantly affect the ablation rate and the bubble formation.[12,17] There is no available evidence, however, to show that the mechanical strength of the thrombus affects the bubble dynamics. This study provided evidence that the mechanical strength of the ablation targets affects the bubble dynamics and suggests that the mechanical strength of the thrombus should be considered when modeling the bubble dynamics during laser thrombolysis and photomechanical drug delivery.

The bubble behavior becomes closer to that formed on solid targets.[4] Bubble oscillation was observed for bubbles formed on a harder gelatin as shown for a 3.5% 300 bloom gel in Fig. 8. The ejection of materials always followed the bubble collapse for bubbles formed on a soft gelatin (e.g., 3.5% 60 bloom gel), as shown in Fig. 7. The bubble shape was also affected by the mechanical strength. For example,

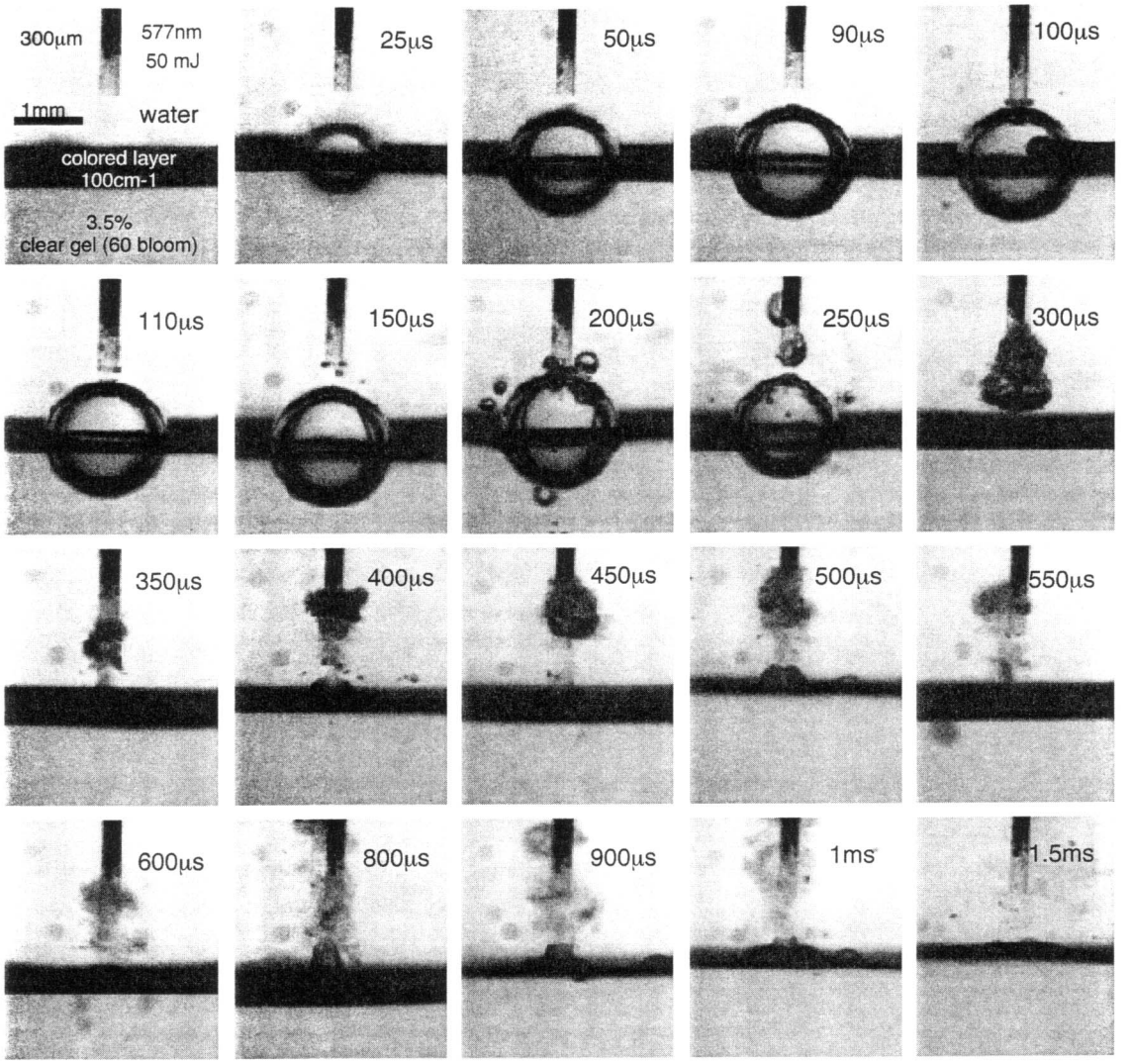

Fig. 7 Flash photographs in side view of bubble growth and collapse on an absorbing gelatin surface after the laser pulse. Single pulses of 50 mJ were delivered onto absorbing gelatin surface (3.5% 60 bloom, 100 cm^{-1}) through clear water via a 300-μm fiber. The fiber tip was placed 1 mm above the gelatin surface.

bubbles formed on soft gelatin kept an almost spherical shape until collapse (Fig. 9), and those formed on harder gelatin were pushed back to the surface due to the resistance from the gelatin (Fig. 10). The maximal bubble volume was similar for both cases although the bubble dynamics were significantly different. A possible explanation for these phenomena was that the bubble had enough energy to overcome the resistance from the harder gelatin during the expansion phase, and then the pressure inside the bubble decreased rapidly and eventually became smaller than the resistance and pressure of the surrounding liquid. Consequently, the bubble was pushed back to the surface, since the resistance from the water above the gelatin surface was much smaller than that from the gel.

5 Implications

This study suggests that photomechanical drug delivery can be achieved selectively by using different strategies to generate the laser-induced hydrodynamic pressures in fluid-filled vessels. One strategy is to generate bubbles on the thrombus due to the absorption of laser energy by the thrombus in coincidence with the injection of drug. In this case, the effect of drugs with different physical properties on the bubble formation will be negligible. The other method is to create bubbles in surrounding liquids (saline or blood), and the bubble dimension can be controlled by either the properties of the fluids or by using different laser parameters.

It has been shown that the rapidly expanding and collapsing bubble induced by pulsed-dye laser radiation can cause perforation, dissection, and other unwanted tissue effects.[18,15] The hydrodynamic pressures arising for the bubble expansion and collapse, however, could be harnessed under controlled circumstances for photomechanical drug delivery. Currently, two strategies to reduce the bubble dimensions are clinically used. One of the strategies is called multiplexing.[19] This method uses a multifiber catheter to generate a number (8 to 12) of smaller laser pulses (with the same radiant exposure) by consecutively delivering laser pulses at different sectors of the catheter. The

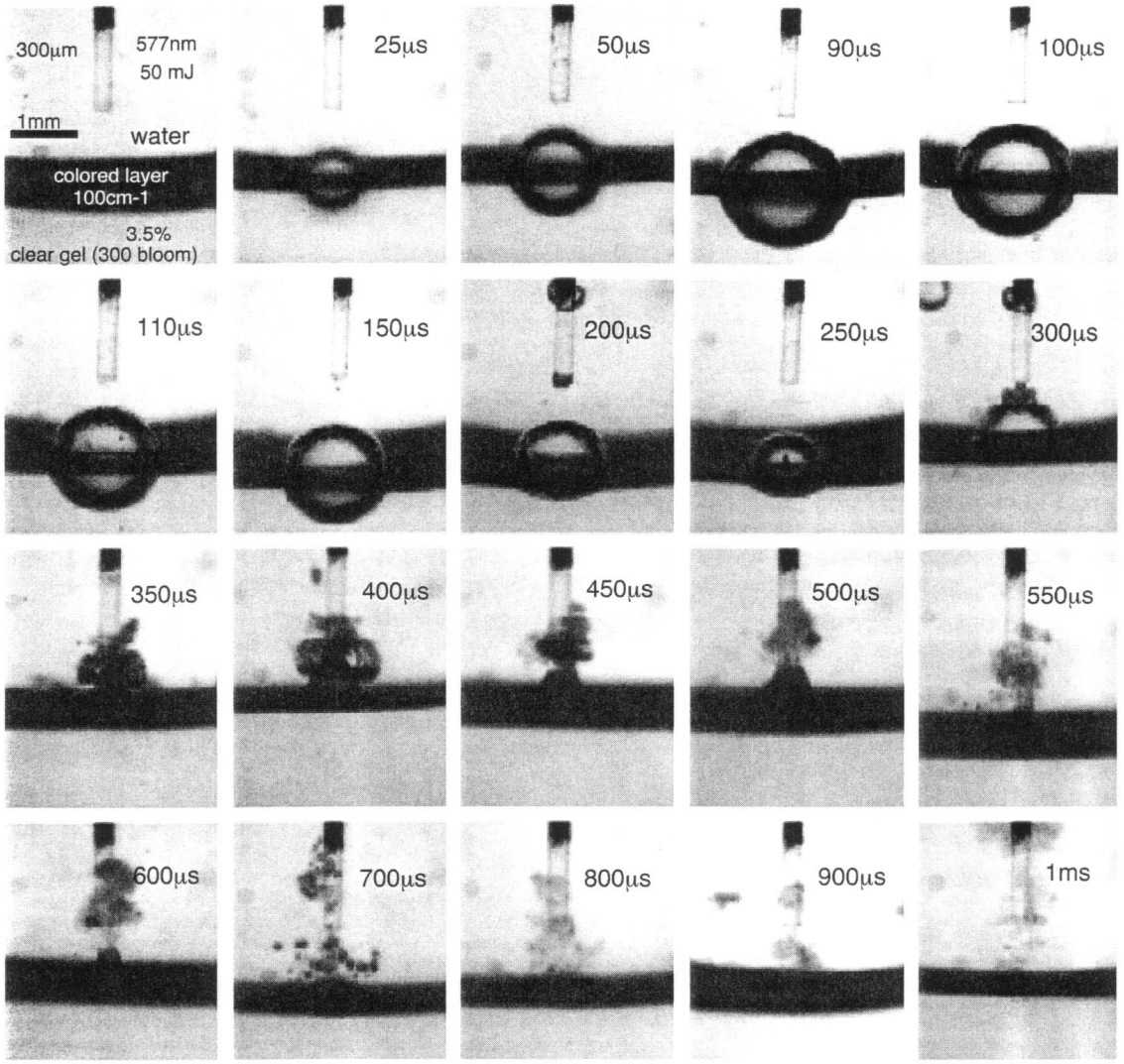

Fig. 8 Flash photographs in side view of bubble growth and collapse on an absorbing gelatin surface after the laser pulse. Single pulses of 50 mJ were delivered onto absorbing gelatin surface (3.5% 300 bloom, 100 cm^{-1}) through clear water via a 300-μm fiber. The fiber tip was placed 1 mm above the gelatin surface.

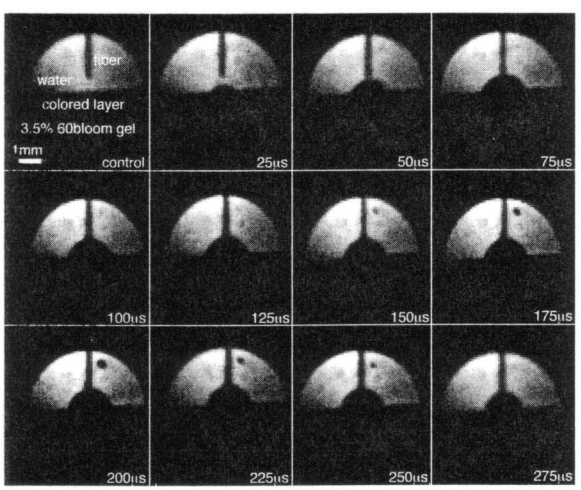

Fig. 9 Shadowgraphs of bubble formation on the 100-cm^{-1} gelatin sample (3.5% 60 bloom). Single pulses of 50 mJ were delivered onto the gelatin surface through clear water via a 300-μm fiber. The fiber tip was 1 mm above the surface.

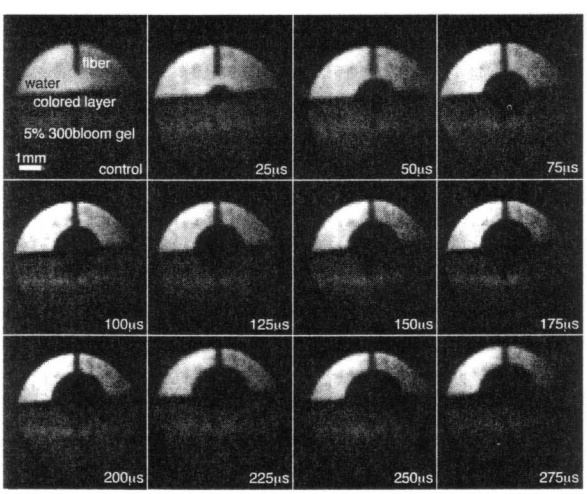

Fig. 10 Shadowgraphs of bubble formation on the 100-cm^{-1} gelatin sample (5% 300 bloom). Single pulses of 50 mJ were delivered onto the gelatin surface through clear water via a 300-μm fiber. The fiber tip was 1 mm above the surface.

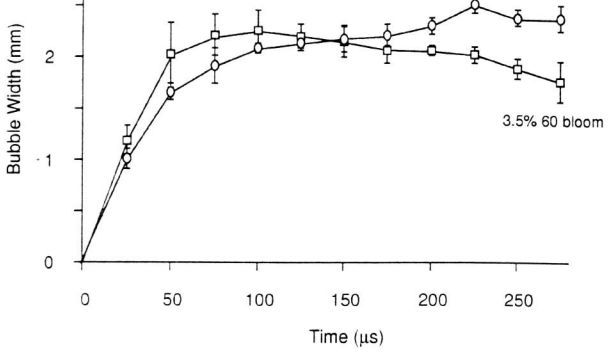

Fig. 11 Bubble width as function of time after the laser pulse for 3.5% 60-bloom gelatin and 5% 300-bloom gelatin. Error bars represent the standard deviation of three measurements.

other method is to dilute the blood by applying a saline flush during the laser procedure.[20] Moreover, a recent study by Vogel et al. suggested that cavitation-induced dilation of vessel walls occurring in pulsed laser angioplasty can be prevented by division of the laser pulse energy into a prepulse with low energy and an ablation pulse with high energy.[16]

This study provides evidence that bubbles of the same size could result in similar hydrodynamic pressures. This finding demonstrates that a small fiber could be used to create the same displacement of intravascular fluids with lower energy as that created by a larger fiber with higher energy.

6 Conclusion

Experimental evidence has shown that similar hydrodynamic pressures could be generated using a small fiber with lower energy rather than using a larger fiber with higher energy. The bubble formation was relatively independent of the liquid properties when the bubbles were formed on the ablation targets under clear liquids. The bubble formation in absorbing liquids strongly depended on the material properties. The mechanical strength of the ablation targets affected the bubble geometry, and the bubble became more elliptical after it reached its maximal dimension for the harder targets. The high-speed shadowgraphs showed that the series of individual stroboscopic pictures could be used for the characterization of the cavitation events, although it took at least 12 times longer to photograph the process using the flash photographic setup than using a high-speed electronic framing camera.

Acknowledgments

The authors wish to thank Dr. K. W. Gregory and A. Shearin for their generous support during this project, Dr. R. P. Godwin and Dr. R. E. Hermes of the Los Alamos National Laboratory for their valuable discussion, and D. B. Stahl at the Los Alamos National Laboratory for assistance with high-speed shadowgraphy. This work was sup-

References

1. Y. Tomita and A. Shima, "Mechanisms of impulsive pressure generation and damge pit formation by bubble collapse," *J. Fluid Mech.* **169**, 535–564 (1986).
2. R. G. Brewer and K. E. Rieckhoff, "Stimulated Brillouin scattering in liquids," *Phys. Rev. Lett.* **13**, 334–336 (1964).
3. A. Vogel, S. Busch, K. Jungnickel, and R. Birngruber, "Mechanisms of intraocular photodisruption with picosecond and nanosecond laser pulses," *Lasers Surg. Med.* **15**, 32–43 (1994).
4. K. Rink, G. Delacrétaz, and R. P. Salathé, "Fragmentation process of current laser lithotriptors," *Lasers Surg. Med.* **16**, 134–146 (1995).
5. K. Gregory, "Laser Thrombolysis," Chap. 53 in *Interventional Cardiology*, Vol. 2, E. J. Topol, Ed., pp. 892–902, W. B. Saunders, Philadelphia (1994).
6. H. Shangguan, L. W. Casperson, A. Shearin, K. W. Gregory, and S. A. Prahl, "Drug delivery with microsecond laser pulses into gelatin," *Appl. Opt.* **35**, 3347–3357 (1996).
7. H. Shangguan, "local drug delivery with microsecond laser pulses: *In vitro* studies," Ph.D. thesis, Portland State University (1996).
8. K. W. Gregory and R. R. Anderson, "Liquid core light guide for laser angioplasty," *IEEE J. Quantum Electron.* **26**, 2289–2296 (1990).
9. U. S. Sathyam, A. Shearin, E. A. Chasteney, and S. A. Prahl, "Threshold and ablation efficiency studies of microsecond ablation of gelatin under water," *Lasers Surg. Med.* **19**, 397–406 (1996).
10. A. Vogel, W. Lauterborn, and R. Timm, "Optical and acoustic investigations of the dynamics of laser-produced cavitation bubbles near a solid boundary," *J. Fluid Mech.* **206**, 299–238 (1989).
11. T. G. van Leeuwen, E. D. Jansen, A. J. Welch, and C. Borst, "Excimer laser induced bubble: Dimensions, theory, and implications for laser angioplasty," *Lasers Surg. Med.* **18**, 381–390 (1996).
12. E. D. Jansen, T. Asshauer, M. Frenz, M. Motamedi, G. Delacrétaz, and A. J. Welch, "Effect of pulse duration on bubble formation and laser-induced pressure waves during holmium laser ablation," *Lasers Surg. Med.* **18**, 278–293 (1996).
13. Y. C. Fung, *Biomechanics—Mechanical Properties of Living Tissues*, 2nd ed., Springer, Berlin (1993).
14. Lord Rayleigh, "On the pressure developed during the collapse of a spherical cavity," *Phil. Mag.* **34**, 94–98 (1917).
15. R. de la Torre and K. W. Gregory, "Cavitation bubbles and acoustic transients may produce dissections during laser angioplasty," *J. Am. Coll. Cardiol.* **19A**, 48 (1992).
16. A. Vogel, R. Engelhardt, U. Behnle, and U. Parlitz, "Minimization of cavitation effects in pulsed laser ablation—illustrated on laser angioplasty," *Appl. Phys. B* **62**, 173–182 (1996).
17. J. T. Walsh Jr. and T. F. Deutsch, "Pulsed CO_2 laser ablation of tissue: effect of mechanical properties," *IEEE Trans. Biomed. Eng.* **36**, 1195–1201 (1989).
18. K. W. Gregory, M. R. Prince, G. M. LaMuraglia, T. J. Flotte, L. Buckley, J. M. Tobin, A. A. Ziskind, J. Caplin, and R. R. Anderson, "Effect of blood upon the selective ablation of atherosclerotic plaque with a pulsed dye laser," *Lasers Surg. Med.* **10**, 533–543 (1990).
19. M. Oberhoff, S. Hassenstein, H. Hank, D. Y. Xie, E. Blessing, A. Baumbach, S. Hanke, K. K. Betz, and K. R. Karsch, "Smooth excimer laser coronary angioplasty (SELCA)—initial experimental results," *Circulation* **86**(Suppl. I, abstract), I-800 (1992).
20. F. Litvack, N. L. Eigler, and J. R. Margolis, "Percutaneous excimer laser coronary angioplasty," *Am. J. Cardiol.* **66**, 1027–1032 (1990).

HanQun Shangguan received the BEng degree in optical instrumentation from Wu-Han Institute of Surveying and Mapping, China, in 1982, and the MS and PhD degrees in electrical engineering from Portland State University, Portland, Oregon, in 1993 and 1996, respectively. From 1982 to 1990, he was an engineer at China Nuclear Instruments and Equipment Co., China. He has been with Oregon Medical Laser Center since 1991. His current research interests are in light delivery systems for photodynamic therapy and tissue weld, fluorescence spectroscopy, laser-induced cavitation bubble dynamics, and drug delivery with microsecond laser pulses. He has over 20 research publications. Dr. Shangguan is a member of Eta Kappa Nu and the Optical Society of America.

Lee W. Casperson received the BS degree in physics from the Massachusetts Institute of Technology, Cambridge, in 1966, and the MS and PhD degrees in electrical engineering and physics from the California Institute of Technology, Pasadena, in 1967 and 1971, respectively. From 1971 to 1983, he was a faculty member in the Department of Electrical Engineering at the University of California, Los Angeles, and since 1983, he has been with the Department of Electrical Engineering at Portland State University, Portland, Oregon. His current research interests are in lasers and optical systems. He has over 200 research publications. Dr. Casperson was awarded the IEEE Centennial Medal and is a fellow of IEEE and the Optical Society of America.

Dennis L. Paisley: Biography and photograph appear with the guest editorial in this issue.

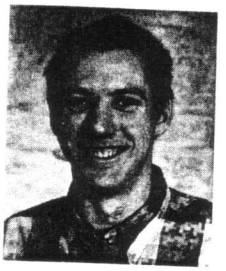

Scott A. Prahl received the BS degree in physics from the California Institute of Technology, Pasadena, in 1982, and the PhD degree in biomedical engineering from the University of Texas, Austin, in 1988. From 1990 to 1991, he was an instructor in Wellman Laboratories at Massachusetts General Hospital, Boston. Since 1992, he has been with the Oregon Medical Laser Center, the Department of Electrical Engineering, Oregon Graduate Institute, Portland, Oregon, and the Department of Dermatology, Oregon Health Sciences University, Portland. His current research interests are in noninvasive measurement of subsurface temperature, visible and infrared spectroscopy of tissues, and tissue optics. He is the author of over 100 research publications. Dr. Prahl was the recipient of the Dermatology Foundation Research Award. He is a fellow of the American Society for Laser Medicine and Surgery.